

Accuracy and efficacy of percutaneous biopsy and ablation using robotic assistance under computed tomography guidance: a phantom study

Yilun Koethe · Sheng Xu · Gnanasekar Velusamy ·
Bradford J. Wood · Aradhana M. Venkatesan

Received: 25 July 2013 / Revised: 24 September 2013 / Accepted: 10 October 2013
© European Society of Radiology (outside the USA) 2013

Abstract

Objective To compare the accuracy of a robotic interventional radiologist (IR) assistance platform with a standard freehand technique for computed-tomography (CT)-guided biopsy and simulated radiofrequency ablation (RFA).

Methods The accuracy of freehand single-pass needle insertions into abdominal phantoms was compared with insertions facilitated with the use of a robotic assistance platform ($n=20$ each). Post-procedural CTs were analysed for needle placement error. Percutaneous RFA was simulated by sequentially placing five 17-gauge needle introducers into 5-cm diameter masses ($n=5$) embedded within an abdominal phantom. Simulated ablations were planned based on pre-

procedural CT, before multi-probe placement was executed freehand. Multi-probe placement was then performed on the same 5-cm mass using the ablation planning software and robotic assistance. Post-procedural CTs were analysed to determine the percentage of untreated residual target.

Results Mean needle tip-to-target errors were reduced with use of the IR assistance platform (both $P<0.0001$). Reduced percentage residual tumour was observed with treatment planning ($P=0.02$).

Conclusion Improved needle accuracy and optimised probe geometry are observed during simulated CT-guided biopsy and percutaneous ablation with use of a robotic IR assistance platform. This technology may be useful for clinical CT-guided biopsy and RFA, when accuracy may have an impact on outcome.

Key points:

- A recently developed robotic intervention radiology assistance platform facilitates CT-guided interventions.
- Improved accuracy of complex needle insertions is achievable.
- IR assistance platform use can improve target ablation coverage.

Y. Koethe · S. Xu · B. J. Wood · A. M. Venkatesan
Center for Interventional Oncology, NIH Clinical Center, National Institutes of Health, Bethesda, MD, USA

Y. Koethe · B. J. Wood · A. M. Venkatesan
Radiology and Imaging Sciences, NIH Clinical Center, National Institutes of Health, Bethesda, MD, USA

Y. Koethe
Duke University School of Medicine, Durham, NC, USA

G. Velusamy
Perfint Healthcare Pvt. Ltd., Chennai, India

A. M. Venkatesan (✉)
Center for Interventional Oncology, Radiology and Imaging Sciences, NIH Clinical Center, National Institutes of Health, 10 Center Drive, Building 10 CRC, Room 1C369, MSC 1182, Bethesda, MD 20892, USA
e-mail: venkatesana@cc.nih.gov

Keywords Interventional radiology · Robotics · Image-guided biopsy · Ablation techniques

Abbreviations

IR Interventional radiologist
RFA Radiofrequency ablation

Introduction

Percutaneous computed-tomography (CT)-guided interventions can be used effectively for image-guided biopsy and tumour ablation [1]. CT-guided biopsy can effectively obtain samples for histological assessment of a tumour, and is advantageous given its minimally invasive approach and ability to enable visualisation of deep tissues [2]. However, the accuracy of CT-guided needle placement, which influences diagnostic yield, is highly dependent upon physician experience. Vulnerable anatomy (such as bowel, nerves or vessels in proximity to the target) has low tolerance for needle placement errors. With conventional techniques, challenging biopsy targets frequently mandate multiple needle adjustments and intra-procedural imaging, which can prolong procedure duration, and increase patient radiation exposure and procedural risk [3, 4]. Needle-based thermal ablation such as radiofrequency ablation (RFA) induces coagulative necrosis of tumours such as hepatocellular carcinoma, hepatic metastases and renal cell carcinoma [1, 3, 5–8]. While RFA has been shown to achieve results comparable to surgical resection for small tumours, such as hepatocellular carcinomas <3 cm, its efficacy has been shown to be reduced for larger tumours [6, 9, 10]. In addition to greater heat sink effect with larger, more perfused tumours, reduced efficacy of RFA for large tumours may be in part attributable to multi-probe placement complexity, which is prone to human error. This is critical for successful large volume composite ablation, however, in order to achieve ablation of both tumour and an intended tumour-free margin [11, 12].

Navigational software and robotic assistance may offer a tailored solution to physicians confronting a technically challenging biopsy or ablation target. Early phantom and clinical experience with robotic navigation systems suggest procedural accuracy, reduced procedure time and reduced patient radiation exposure compared with freehand techniques [13–19]. Experience with software systems enabling ablation planning has also been favourably described [20, 21]. In this study, an IR assistance platform was evaluated that combines navigational software and robotic guidance to facilitate percutaneous biopsy and ablation probe placement. Needle placement accuracy and ablation efficacy were assessed in abdominal phantoms.

Materials and methods

Robotic IR assistance platform device

Device specifications, emergency options

The robotic IR assistance platform (MAXIO; Perfint Healthcare, Chennai, India) has dimensions of 850 mm ×

800 mm × 1,350 mm (length × width × height) in the parked position) and 850 mm × 800 mm × 1,800 mm when docked at the CT table side, with the robotic arm positioned over the CT table. The weight of the device is 250 kg and it is propelled via four way swivel wheels. The device requires between approximately 3–4 min total to be physically moved from its parked position to CT table side, to dock the device and boot it up. It requires approximately the same amount of time to switch off the device, undock and move it to the parking location identified inside the CT suite. The device's robotic arm takes approximately 30–45 s to move from its initial position to the position to clamp the needle guide.

Two emergency shut off functions are available for this device. One is an emergency switch physically located on the robotic arm, whose actuation will stop all device axis movement. If the needle guide is already clamped the device will release the clamped needle holder immediately and the device will be restored to a “safe state”, during which all the movement related components of the device are stopped and no further movement is possible before intervention by the user to reset the position values and command the device to move again. The device also has a Cancel Movement option in the software which the user may click on using the device's track pad. This will also stop all movements and restore the device to its “safe state”.

Physical docking, optical registration and DICOM data retrieval

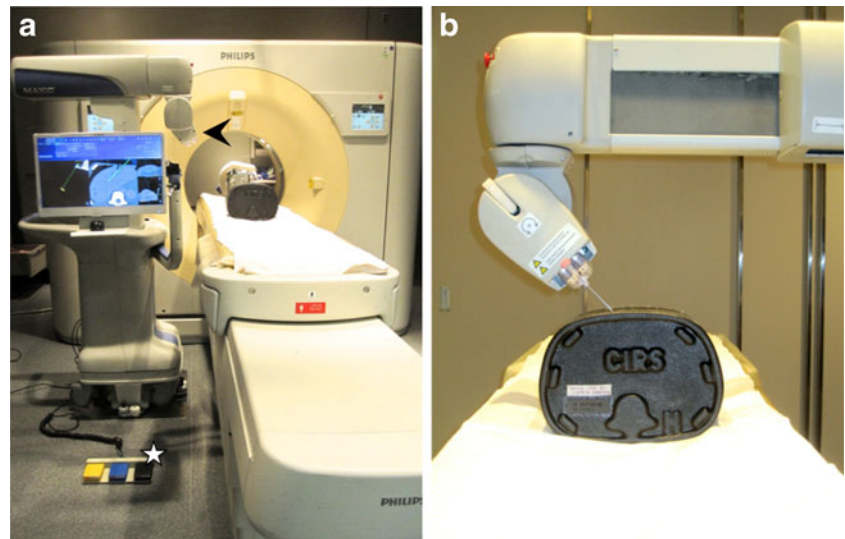
Registration between the robotic IR assistance platform and the CT table occurs via a mechanical docking mechanism, optical registration and tilt sensing (MAXIO; Perfint, Chennai, India) (Fig. 1a). Provided all three components of registration (mechanical docking, optical registration and tilt sensing) are successfully executed, the platform permits procedures to be carried out. Consistent docking and registration of the robotic device abrogates the need for robot-to-CT registration with each use. The platform's computer console receives DICOM formatted images from the CT console via an Ethernet cable, and displays the images on its planning and navigation software.

Biopsy and ablation planning software

The system has a track pad for the user to interact with the computer. Using the track pad, the physician selects the needle or probe type and length from a series of drop-down menus on the computer console integrated into this device. Needle/probe trajectory and biopsy or ablation target are selected directly on the DICOM data transferred to the device's computer console.

DICOM CT data may be displayed in the axial as well as sagittal and coronal planes by the graphical user interface. The physician operator plans a biopsy with the navigational

Fig. 1 Robotic interventional radiologist (IR) assistance platform set-up. **a** The robotic arm at baseline position (*black arrowhead*). Foot pedals (*white star*) can be used to initiate robotic arm movement and opening and closing of the end effector. Planning of percutaneous interventions are carried out and displayed on the monitor of the platform's computer console. **b** Robotic arm end effector grips onto the inserted needle guide before needle insertion



software by selecting the intended probe type and length, then selecting the target and skin entry site directly on the DICOM imaging data (Fig. 2). After these inputs, the system software subsequently instructs the operator to move the CT table to a prescribed z -axis location. It then prescribes the trajectory to the robotic arm. For ablation planning, the physician segments the target by using the track pad to hover the computer cursor over the target on pre-procedural CT. Based on differences in voxel intensity, the software generates a preliminary segmentation on multi-planar reformatting images and a three-dimensional (3D) reconstruction. If necessary, the physician manually edits the segmentation until satisfactory. The physician can subsequently plan the ablation by dictating the probe type and trajectory. The platform displays a

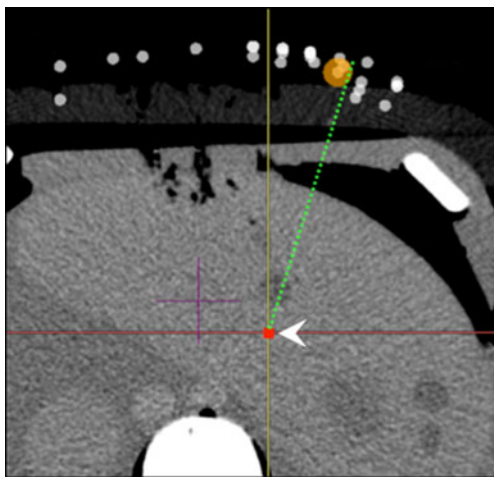


Fig. 2 Single-pass needle insertion planning using an IR assistance platform. Point target is delineated (*white arrowhead*) on axial images as well as reconstructed coronal and sagittal images (not pictured). Simulated needle trajectory is displayed as a *dotted line* on anatomical images

simulated composite ablation zone over the axial, reconstructed coronal and reconstructed sagittal images, and co-displays the target and superimposed ablation geometry on the 3D reconstructions (Fig. 3). As the operator adds additional probes to the composite ablation plan, the ablation planning software updates the displayed ablation zone to reflect additional probe contributions to the total ablation volume.

Robotic assistance for biopsy/ablation

The computer console communicates with the robotic guide arm via an RS232 interface to move according to the physician dictated plan. The robotic guide arm possesses 5 degrees of freedom and is able to achieve needle insertions up to 230 mm from the gantry centre line to the side opposite that of the docked device. Those needle angles or skin entry sites outside of this range mandate installation of another floor mounted docking plate on the other side of the examination table and physical docking of the robotic on the contralateral table side. Once the robotic arm has moved to the correct location, the physician operator instructs the end effector of the robotic guide arm via the computer console to grip a plastic, gauge-specific needle guide (Fig. 1b). The physician then manually inserts the needle through the needle guide until the needle hub contacts the needle guide. Once the needle is in place, the physician instructs the robotic device to unclamp its end effector and withdraw its robotic arm from the procedural site.

Experimental set-up

The IR assistance platform was physically docked on the right side of the CT table (Philips Brilliance iCT; Philips

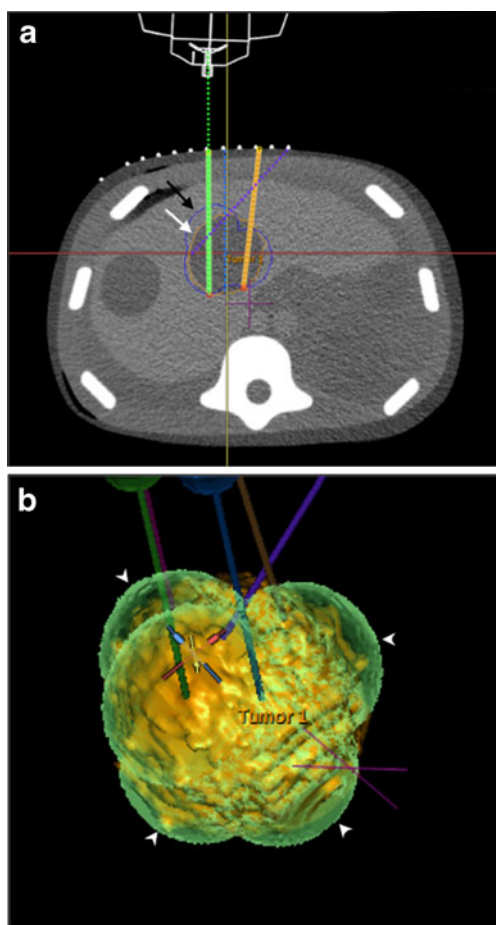


Fig. 3 Ablation planning on an IR assistance platform. Ablation planning software displays axial images (**a**) as well as reconstructed coronal and sagittal images (not pictured). After tumour segmentation (segmented tumour: *white arrow*, **a**), probes are planned and their trajectories displayed on the anatomical images (probes: *solid/dotted lines* in **a**). The predicted composite ablation zone is superimposed onto the segmented tumour on both multiplanar images and on a 3D shaded surface display (composite ablation zone: *black arrow* in **a**, *white arrowheads* in **b**)

Healthcare, Cleveland, OH, USA) (Fig. 1). Image acquisition properties were based on the manufacturer's recommendations (5-mm section thickness, 1-mm reconstruction interval). Optically opaque abdominal phantoms (Triple Modality 3D Abdominal Phantom Model 057; CIRS, Norfolk, VA, USA) were used for needle and probe placement. All needle insertions were performed by an attending interventional radiologist with 7 years of percutaneous biopsy and ablation experience.

Needle placement for biopsy

Twenty pairs of virtual point targets and skin entry points with a mean entry-to-target distance of 11.0 cm (range, 10.2–11.5 cm) were selected on pre-procedural CT using custom software (intGuide; National Institutes of Health, Bethesda,

MD, USA). Each pair of target and skin entry points comprised a complex multi-angle needle trajectory with angular deviations in the x , y and z directions. Single-pass needle insertions were performed using an 18-gauge, 15-cm needle (Biomedical SRL, Firenze, Italy). Insertions were first performed using a freehand technique, employing only the CT gantry laser light and the markings of the CT grid placed over the phantom during pre-procedural imaging and for localisation (Fast Find Grid; Webb Manufacturing Corporation, Philadelphia, PA, USA). Insertions were subsequently performed with the use of the IR assistance platform. Neither intra-procedural needle adjustments nor intra-procedural CTs were permitted for either approach.

Needle placement for composite ablation simulation

Custom opaque abdominal phantoms (CIRS, Norfolk, VA, USA) were designed containing multiple 5-cm diameter embedded masses meant to simulate 3-cm diameter tumours and surrounding 1-cm tumour-free margins. For each target, five simultaneous RFA electrode placements were planned with the intent of maximising simulated ablation of the target (i.e. simulated tumour and tumour-free margin). A total of five 17-gauge, 15-cm needle introducers (Cardinal Health, Dublin, OH, USA), simulating 15-cm long, 3-cm active tip CoolTip RFA Electrodes (Covidien, Dublin, Ireland), were inserted into the 5-cm diameter embedded targets. Ablations were first planned manually on the CT console after obtaining an initial CT of the phantom. Needle insertions were then executed freehand, employing only the CT gantry laser light and the markings of the CT grid placed over the phantom during pre-procedural imaging for localisation. Probe placement was subsequently planned and executed using the IR assistance platform's ablation planning software. Neither needle adjustments nor intra-procedural CTs were permitted between needle insertions. Post-procedural imaging documenting needle locations and positions was obtained subsequent to needle placement for each technique.

Image analysis

Custom software (intGuide; National Institutes of Health, Bethesda, MD USA) was used to select the needle tip on the post-procedural CTs obtained after biopsy needle insertion. The custom software subsequently calculated the Euclidian distance between the tip of the needle and the virtual target, corresponding to the "tip-to-target distance."

Custom research software (OncoNav; National Institutes of Health, Bethesda, MD, USA) derived from Medical Image Processing, Analysis and Visualization (MIPAV) software (National Institutes of Health) was employed for simulated ablation analysis [22]. The target was manually segmented, and each needle displayed on post-procedural CT was

manually outlined. Ablation zone geometry and size was subsequently predicted based on needle placement and manufacturer-prescribed ablation size (3.6×3.7 cm ellipsoidal coverage per needle) [23]. The software subtracted the composite ablation volume from the segmented target volume thereby calculating the percentage residual non-ablated target (Fig. 4).

Statistics

Paired *t*-tests were used to compare the differences in needle tip-to-target distance for simulated biopsy. Paired *t*-tests were also used to compare the differences in percentage residual target for simulated ablation. 95 % confidence intervals were assumed ($\alpha \leq 0.05$). Descriptive statistics were employed to calculate mean entry-to-target distance and mean angular deviation for simulated biopsy.

Results

Mean entry-to-target distance was 11.0±3.8 cm (range, 10.2–11.5 cm) for needle insertions simulating percutaneous biopsy. A shorter mean needle tip-to-target distance was observed with use of the IR assistance platform compared with the freehand technique (6.5±2.5 mm vs 15.8±9.2 mm, respectively; $P < 0.0001$; Fig. 5a). Mean absolute angular deviation off the *z*-axis was 53° (range -68° to 74°). Mean

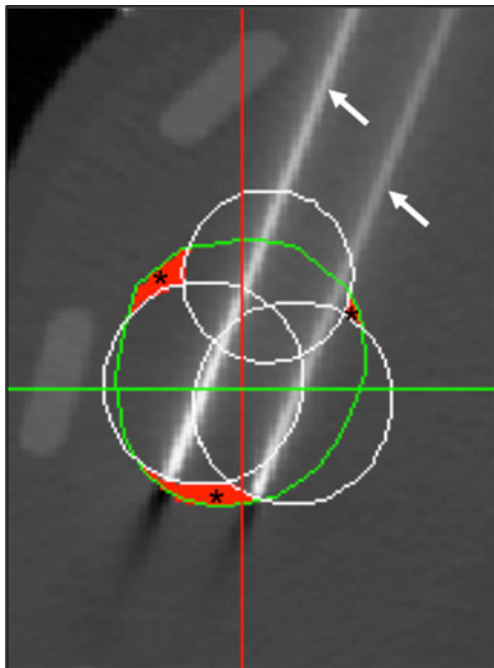


Fig. 4 Analysis of ablation coverage. Representative image demonstrates residual target volume (black asterisks) and ablated volumes (white ovals) around inserted needles (white arrows)

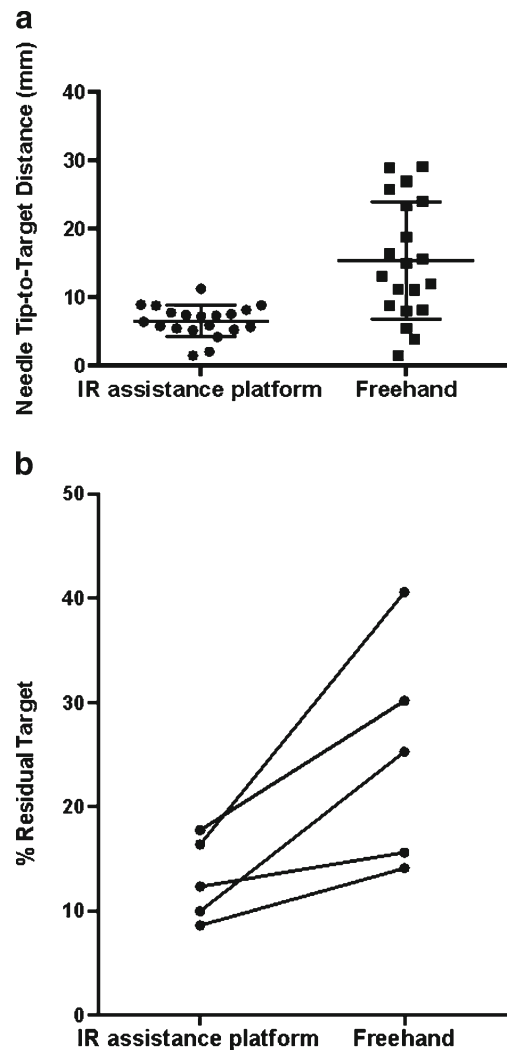


Fig. 5 Scatter plots demonstrate the distribution of tip-to-target distance (a) for freehand and IR assistance platform-guided needle insertion. b Before-after plots demonstrate percentage residual tumour for each target using the freehand technique and the IR assistance platform

absolute angular deviation off the *y*-axis was 46° (range -42° to 56°).

For simulated composite ablation, a lower average percentage of residual target was observed with use of the IR assistance platform (13.0±4.0 %) compared with the freehand technique (25.1±10.9 %; $P = 0.03$; Fig. 5b).

Discussion

In this study, we evaluated the accuracy and efficacy of an integrated IR assistance platform for multi-angle needle placements and ablation planning. Improved needle accuracy compared with freehand technique was demonstrated with the use of this IR assistance platform for challenging, single-pass, multi-angle needle trajectories.

Improved needle placement accuracy may clinically translate into decreased complication rates and greater sampling success for biopsies [6, 9, 10, 24]. Out-of-plane trajectories have traditionally been challenging to plan with CT guidance. If the entry point and the target are in two different planes, only one can be visualised at a time, making it challenging to plan multi-angle trajectories. Compared with traditional CT guidance, cone beam CT or fluoroscopically guided interventions offer an advantage of enabling orthogonal and oblique projections of the skin entry site and target [11, 17]. With this novel IR assistance platform, the challenges of multi-angle visual planning are further circumvented. The skin entry and the target points can be directly planned on the computer console of the IR assistance platform, which subsequently executes the planned trajectory, without requiring physician calculations of entry-to-target distance and angulation.

Reduced variability of needle placement accuracy was also noted with IR assistance platform guidance compared with the freehand technique. A potential explanation for this observation is that freehand needle accuracy is dependent upon physician comfort and skill with a particular angulation and insertion depth, whereas the IR assistance platform does not face this limitation, being presumably equally accurate for both simple and complex angles. Although not evaluated in this study, a novice with limited experience in executing complex multi-angle trajectories might be able to acquire visual, and some tactile experience, by first executing the trajectory with use of this IR assistance platform. The platform's role as a training tool remains an interesting area for further investigation. While treatment planning is frequently used in image-guided external beam radiation therapy and brachytherapy, ablation zone simulation and planning for interventional oncology remains relatively novel [25]. In this study, the use of the ablation planning component of this IR assistance platform was associated with greater target coverage and reduced residual target compared with the freehand technique.

One limitation of the ablation planning component of this platform that should be noted is that the simulated ablation volumes are manufacturer-predicted isotherms, derived largely from *ex vivo* data. The actual ablation volume may vary depending on tissue type, energy source, electrode, and local microscopic and regional perfusion factors [26].

Navigation and guidance tools have the potential to mitigate imperfect operator spatial awareness and hand-eye coordination. Non-robotic navigation and guidance devices that assist physicians include electromagnetic (EM) tracking, optical tracking, laser guidance and cone beam CT fusion. Optical and EM tracking provide information on real-time needle position and orientation, but mandate the use of costly disposables such as EM or optically tracked needles [27, 28]. In addition, they may require extensive pre-procedural

registration, which can be consuming as the location of fiducial markers and EM field generators (or cameras for optical tracking) must be accommodated intra-procedurally [13–17, 29]. Laser guidance has no physical needle guide to steady the needle during insertion. Cone beam CT fusion requires installation of a C-arm and other hardware that may occupy an entire IR suite.

The IR assistance platform used in this study, in comparison, requires minimal time for docking and registration. Like other robotic devices, it can also accurately orientate and guide multi-angle needle insertions without necessitating the use of custom needles. Schulz et al. [17] have recently described a robotic device that assists percutaneous needle insertion for cone beam CT and fluoroscopy-guided procedures (iSYS 1; iSYS Medizintechnik, Kitzbuehel, Austria). This device is mounted to a small platform beneath the CT table, and has 4 degrees of freedom. A phantom study employing this device demonstrated that accurate needle placement can be achieved in a timely manner (average error, 1.1 mm; average duration of procedure, 3:59 min). Solomon et al. [13] and Patriciu et al. [14] have also recently described a robotic system with a total of 11 degrees of freedom that is mounted on a large frame attached to and overlying the CT table (PAKY-RCM; Johns Hopkins, Baltimore, MD, USA). This device has a rolling dowel mechanism that can advance a needle without physician assistance. Use of this device for percutaneous interventions demonstrated accuracy (average error, 1.7 mm), reduced overall procedure time, number of probe passes, and patient and physician radiation exposure compared with conventional techniques.

Compared with other robotic devices for image-guided interventions, this IR assistance platform also has a large range of achievable needle angles, ranging from -90° to 90° in both lateral and craniocaudal directions, provided installation of floor mounted plates and docking on either site of the examination table has been enabled. The automated aspect of this system's robotic arm offers additional unique advantages. Whereas the robotic guide arm of other existing devices must be manually positioned in the vicinity of the target before subsequent end effector localisation is achieved automatically or via joystick use, the robotic guide arm of this platform automatically moves from its docked position to the skin entry point based on the physician dictated plan [17, 20, 21, 30]. As this platform abrogates the need for manual movement of the device after initial registration and docking, the physician can focus on the biopsy and ablation planning steps instead of manually moving the robot during the procedure. Additional advantages of this platform include its mobility, as it can be wheeled away from the CT when not in use.

The limitations of this robotic platform are similar to those of other robotic guidance devices. Once docked, this platform

limits physical access on one side of the CT table near the gantry. In addition, physical docking of the device limits the overall range of craniocaudal targets that are accessible. Another limitation is the fact that tactile experience diminished when using this device, as the needle holder clamps tightly around the needle. Furthermore, as we only report a phantom study, we were not able to evaluate this technique in the *in vivo* environment, when specific challenges like target, patient and respiratory motion must be surmounted. But in this initial study phantom study, we were interested to evaluate the ability of this system to facilitate complex needle angle insertions compared with an experienced operator's freehand single pass insertion. It should also be noted that a single pass needle insertion is not the standard procedure for complex clinical needle placements. It would be of interest to pursue a follow-up study wherein the operator was permitted multiple needle angle adjustments with a series of CT check images to reach a point target, thereby allowing us to compare both needle tip-to-target accuracy as well as radiation dose for freehand versus robotically assisted techniques.

It is arguably difficult to compare the results of this study with those of existing studies describing robotic device use for percutaneous interventional procedures, as each published study has evaluated different endpoints in different ways. Some devices have demonstrated smaller tip-to-target distance compared with the IR assistance platform employed in this study. However, this could be explained by differences in experimental design or the phantom used. Our experimental design called for challenging multi-angle trajectories. Descriptive analysis revealed that all trajectories chosen had challenging angulations with a minimum of 33° of absolute deviation both from *z*-axis and from the midline, and a minimum needle depth of 10 cm. Studies employing other robotic devices have described use of smaller needle angles, which may be in part due to the smaller range of angles achievable with these devices [17].

In conclusion, results from the use of this novel IR assistance platform suggest that it might play a promising role for percutaneous CT-guided biopsies and ablations. Its use was associated with improved needle placement accuracy for complex, multi-angle trajectories and greater ablation coverage for large targets compared with the freehand technique. Future studies are needed to evaluate the role of this IR assistance platform in the clinical setting and to determine its effect on radiation exposure, patient risk and clinical outcome.

Acknowledgements A year-long research fellowship for Y.K. was made possible through the National Institutes of Health (NIH) Medical Research Scholars Program, a public-private partnership supported jointly by the NIH and generous contributions to the Foundation for the NIH from Pfizer Inc., The Leona M. and Harry B. Helmsley Charitable Trust, and the Howard Hughes Medical Institute, as well as other private

donors. For a complete list, please visit the Foundation website at <http://www.fnih.org/work/programs-development/medical-research-scholars-program>). The content of this publication does not necessarily reflect the views or policies of the Department of Health and Human Services, nor does mention of trade names, commercial products, or organizations imply endorsement by the U.S. Government.

X.S.: No potential conflicts of interest to disclose.

G.V. is a full-time salaried employee (Principle Systems Architect, ATO) of Perfint Healthcare Pvt. Ltd. Perfint Healthcare owns intellectual property related to technologies used in this published work, including USPTO # US20130072784, US20120190970, US20130085380, etc. For detailed information, please visit the company website, www.perfinthealthcare.com.

B.J.W. and A.M.V: This research was supported by the NIH Intramural Research Program and the NIH Center for Interventional Oncology. The interventional radiologist assistance platform was supplied by Perfint Healthcare Pvt. Ltd. (Chennai, India) under a Materials Transfer Agreement between the NIH Center for Interventional Oncology and Perfint Healthcare. NIH and Perfint Healthcare have discussed details of a draft Cooperative Research and Development Agreement (CRADA). The content does not necessarily reflect the views or policies of the Department of Health and Human Services, nor does mention of trade names, commercial products or organisations imply endorsement by the U.S. Government.

References

1. Wood BJ, Ramkaransingh JR, Fojo T et al (2002) Percutaneous tumor ablation with radiofrequency. *Cancer* 94:443–451
2. Chintapalli KN, Montgomery RS, Hatab M et al (2012) Radiation dose management: part 1, minimizing radiation dose in CT-guided procedures. *AJR Am J Roentgenol* 198:W347–W351
3. Magnusson A, Akerfeldt D (1991) CT-guided core biopsy using a new guidance device. *Acta Radiol* 32:83–85
4. Onik G, Cosman ER, Wells THJ et al (1988) CT-guided aspirations for the body: comparison of hand guidance with stereotaxis. *Radiology* 166:389–394
5. Bertot LC, Sato M, Tateishi R et al (2011) Mortality and complication rates of percutaneous ablative techniques for the treatment of liver tumors: a systematic review. *Eur Radiol* 21:2584–2596
6. Tiong L, Maddem GJ (2011) Systematic review and meta-analysis of survival and disease recurrence after radiofrequency ablation for hepatocellular carcinoma. *Br J Surg* 98:1210–1224
7. Salhab M, Canelo R (2011) An overview of evidence-based management of hepatocellular carcinoma: a meta-analysis. *J Cancer Res Ther* 7:463
8. Cirocchi R, Trastulli S, Boselli C et al (2012) Radiofrequency ablation in the treatment of liver metastases from colorectal cancer. *Cochrane Database Syst Rev* 6, CD006317
9. Best SL, Park SK, Yaacoub RF et al (2012) Long-term outcomes of renal tumor radio frequency ablation stratified by tumor diameter: size matters. *JURO* 187:1183–1189
10. Hui GC, Tunçali K, Tatli S et al (2008) Comparison of percutaneous and surgical approaches to renal tumor ablation: metaanalysis of effectiveness and complication rates. *J Vasc Interv Radiol* 19:1311–1320
11. Pleguezuelo M, Marelli L, Misseri M et al (2008) TACE versus TAE as therapy for hepatocellular carcinoma. *Expert Rev Anticancer Ther* 8:1623–1641
12. Minami Y, Kudo M (2011) Radiofrequency ablation of hepatocellular carcinoma: a literature review. *Int J Hepatol* 2011:1–9

13. Solomon SB, Patriciu A, Bohlman ME et al (2002) Robotically driven interventions: a method of using CT fluoroscopy without radiation exposure to the physician. *Radiology* 225:277–282
14. Patriciu A, Awad M, Solomon SB et al (2005) Robotic assisted radio-frequency ablation of liver tumors—randomized patient study. *Med Image Comput Comput Assist Interv* 8:526–533
15. Stoffner R, Augschöll C, Widmann G et al (2009) Accuracy and feasibility of frameless stereotactic and robot-assisted CT-based puncture in interventional radiology: a comparative phantom study. *Rofo* 181:851–858
16. Cleary K, Melzer A, Watson V et al (2006) Interventional robotic systems: applications and technology state of the art. *Minim Invasive Ther Allied Technol* 15:101–113
17. Schulz B, Eichler K, Siebenhandl P et al (2012) Accuracy and speed of robotic assisted needle interventions using a modern cone beam computed tomography intervention suite: a phantom study. *Eur Radiol* 23:198–204
18. Zangos S, Melzer A, Eichler K et al (2011) MR-compatible assistance system for biopsy in a high-field-strength system: initial results in patients with suspicious prostate lesions. *Radiology* 259:903–910
19. Schell B, Eichler K, Mack MG et al (2012) Robot-assisted biopsies in a high-field MRI system—first clinical results. *Rofo* 184:42–47
20. Stoll M, Boettger T, Schulze C, Hastenteufel M (2012) Transfer of methods from radiotherapy planning to ablation planning with focus on uncertainties and robustness. *Biomed Tech (Berl)*. doi:10.1515/bmt-2012-4279
21. Lehmann KS, Frericks BB, Holmer C et al (2011) In vivo validation of a therapy planning system for laser-induced thermotherapy (LITT) of liver malignancies. *Int J Color Dis* 26:799–808
22. McCreedy ES, Cheng R, Hemler PF et al (2006) Radio frequency ablation registration, segmentation, and fusion tool. *IEEE Trans Inf Technol Biomed* 10:490–496
23. Covidien (2009) Cool-tip™ RF ablation system [Pamphlet]. Covidien, Boulder
24. Kobayashi K, Bhargava P, Raja S et al (2012) Image-guided biopsy: what the interventional radiologist needs to know about PET/CT. *Radiographics* 32:1483–1501
25. Solomon SB, Silverman SG (2010) Imaging in interventional oncology. *Radiology* 257:624–640
26. Wood BJ, Locklin JK, Viswanathan A et al (2007) Technologies for guidance of radiofrequency ablation in the multimodality interventional suite of the future. *J Vasc Interv Radiol* 18:9–24
27. Wood BJ, Zhang H, Durrani A et al (2005) Navigation with electromagnetic tracking for interventional radiology procedures: a feasibility study. *J Vasc Interv Radiol* 16:493–505
28. Hong CW, Xu S, Imbesi KL, Wood BJ (2013) Integrated laser-guided CT biopsy. *Clin Imaging*. doi:10.1016/j.clinimag.2013.08.006
29. Wood BJ, Kruecker J, Abi-Jaoudeh N et al (2010) Navigation systems for ablation. *J Vasc Interv Radiol* 21:S257–S263
30. Su L-M, Stoianovici D, Jarrett TW et al (2002) Robotic percutaneous access to the kidney: comparison with standard manual access. *J Endourol* 16:471–475